Acta Materialia 120 (2016) 32–39

Contents lists available at ScienceDirect

Acta Materialia

journal homepage: www.elsevier.com/locate/actamat

Full length article

Pseudogap formation and vacancy ordering in the new perovskite boride Zr_2Ir_6B

Dimitrios Koumoulis [a], Jan P. Scheifers [b, 1], Rachid St. Touzani [b], Boniface P.T. Fokwa [b, **], Louis-S. Bouchard [a, c, *]

[a] Department of Chemistry and Biochemistry, University of California, 607 Charles E. Young Drive East, Los Angeles, CA, 90095, USA
[b] Institut für Anorganische Chemie, Rheinisch-Westfälische Technische Hochschule Aachen, 52056, Aachen, Germany
[c] California NanoSystems Institute at UCLA, 570 Westwood Plaza, Los Angeles, CA, 90095, USA

ARTICLE INFO

Article history:
Received 25 May 2016
Received in revised form
11 August 2016
Accepted 13 August 2016

Keywords:
Electronic pseudogap
Vacancy ordering
Double perovskite
Boride
NMR

ABSTRACT

Non-oxide perovskites exhibit unusual properties such as negative thermal expansion, negative thermal coefficient of resistance, positive and negative giant magnetoresistance as well as superconductivity. These uncommon properties appear to originate from the basic structure only, in strong contrast to the oxides. Ordering in nonstoichiometric compounds may not only lead to different chemical compositions but also to the promotion of these physical properties. We present a combined NMR and first-principles study of the cubic Zr_2Ir_6B perovskite to investigate the boron ordering with boron deficiency leading to the formation of superstructure. Competing ionic and metallic interactions reflect the semimetallic character of this boride and result in the formation of a pseudogap, as predicted by our first principles calculations and verified experimentally by ^{11}B solid state NMR. Several avoided crossing scenarios were also found for the bands from the conducting states at +1 eV to the Fermi level along specific directions. This observation is of paramount importance for understanding the structure-property relationships in metal boride perovskites and the search for new cubic perovskites.

1. Introduction

The simple perovskite structure type ($SrTiO_3$-type) and its derivatives (resulting from cation orderings and octahedra tilting) are the most frequently encountered in solid-state materials research. This is due to the relative simplicity of the basic crystal structure and because of the numerous catalytic and physical properties emerging from this particular structural arrangement [1]. Although the majority of perovskites are oxides, some carbides, nitrides, halides, hydrides and borides also crystallize in this structure. Derivatives of this structure have been observed for the oxide perovskites, and in particular cation ordering studies [2] have led to the family of double perovskites with general formula $A_2BB'O_6$ (A, B, B′ are cations with different sizes) for which numerous properties have emerged including high-temperature itinerant magnetism [3] and room-temperature magnetoresistance [4]. On the other hand, defective perovskite oxides have produced the large family of cuprates showing high-temperature superconductivity, a property related to the presence of a pseudogap in the electronic structure [5].

The non-oxide perovskites (also called anti-perovskites, AM_3X, where A and M are metals and X is either N, C, or B) have not been as extensively studied as their oxides counterparts, although they also exhibit a variety of exciting properties such as negative thermal expansion in $GdPd_3B_{0.25}C_{0.75}$, negative thermal coefficient of resistance for $GdPd_3B$ [6], positive and negative giant magnetoresistance in $TbPd_3B$ and $TbPd_3$, respectively [6], valence instability of Eu in $EuPd_3B_x$[7] and superconductivity in $MgNi_3C$ [8]. These properties seem to originate from the basic structure only, in strong contrast to the oxides. However, nonstoichiometry has often been reported in these phases at the light element sites (AM_3X_y) [9,10], thus a possible ordering would not only lead to different chemical compositions but also to

* Corresponding author. Department of Chemistry and Biochemistry, University of California, 607 Charles E. Young Drive East, Los Angeles, CA, 90095, USA.
** Corresponding author. Department of Chemistry, University of California, Chemical Sciences Building, 501 Big Springs Road, Riverside, CA, 92521, USA.
E-mail addresses: boniface.fokwatsinde@ucr.edu (B.P.T. Fokwa), louis.bouchard@gmail.com (L.-S. Bouchard).
[1] Present address: Department of Chemistry, University of California, Chemical Sciences Building, 501 Big Springs Road, Riverside, CA, 92521, USA.

http://dx.doi.org/10.1016/j.actamat.2016.08.031
1359-6454/

unexpected physical properties. In fact, Yubuta et al. have shown, using selected area electron diffraction (SAED) that the anomaly, a sharp drop of microhardness values near $x = 0.5$ in $ScRh_3B_x$ and $CeRh_3B_x$ series, is directly related to presence of superstructure and satellite reflections [11,12]. This finding indicates a possible structural ordering for these phases and thus the need of a careful crystallographic study of this type of material by X-ray or neutron diffraction for accurate composition-structure determination. Using single-crystal X-ray diffraction, Fokwa et al. discovered such ordering for the first time in Ti_2Rh_6B ($Fm\bar{3}m$, no. 225, vacant double perovskite structure) [13,14], the structure of which contains empty and filled octahedra strictly alternating in a $2 \times 2 \times 2$ super cell (Fig. 1). Also, non-stoichiometric $ZrIr_3B_{0.5}$ known for several decades was reformulated to Zr_2Ir_6B [15], based on powder and single-crystal X-ray diffraction data. It has been shown that the $2 \times 2 \times 2$ superstructure is stable only for a certain regime of valence electrons (VE) between 63 and 68 [16], while the substructure is stable between 31 and 34.5 VE [17] (which would correspond to 62 and 69 VE in the superstructure). Interestingly, the transition from superstructure to simple structure is accompanied by a decrease in the lattice parameter, which remains unexplained [16]. Zeiringer et al. found a similar behavior in the series $CeRh_{3-x}Pd_xB_{0.5}$[18]. For small $x < 1.5$ they observed superstructure reflections via SAED and a decreasing lattice parameter when substituting the smaller Rh with Pd in $CeRh_{1.8}Pd_{1.2}B_{0.5}$ leading to $CePd_3B_{0.5}$. Interestingly, the Zr–Ir distance in Zr_2Ir_6B is ca. 2.83 Å, which is 5% significantly smaller than the sum of the metallic radii [19]. Fifty years ago Holleck [20] pointed out that Sc behaves either like a group III or a group IV metal with a radius of 1.64 Å and 1.52 Å, respectively. However, this is still insufficient to explain the short Ir–Zr distance in Zr_2Ir_6B.

The present study examines the occurrence of the superstructure throughout the sample and its coexistence with the simple cubic structure in Zr_2Ir_6B. The simple cubic structure is not detectable without a suitable reference by means of X-ray diffraction, if it coexists with the superstructure in the sample, because of identical positions of the substructure reflections.

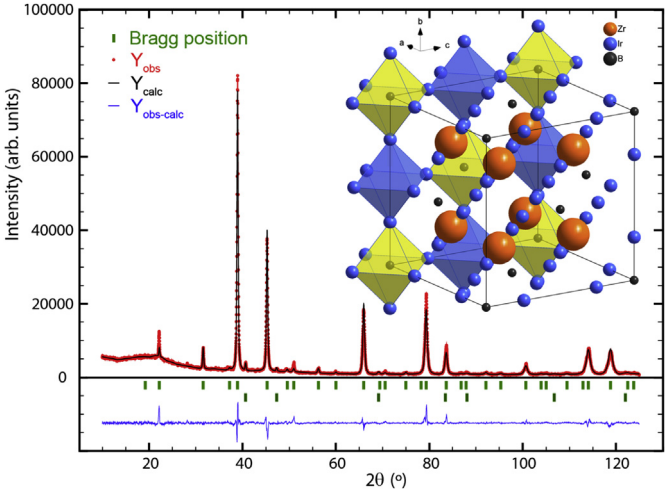

Fig. 1. Crystallographic study of the double perovskite by X-ray. Rietveld refinement of the PXRD pattern (Cu-Kα1 radiation) of Zr_2Ir_6B with a small fraction of Zr-doped iridium. The upper marks indicate the position of the Bragg reflections of Zr_2Ir_6B. The lower marks belong to the Ir phase. The average weight fraction of the Zr_2Ir_6B is about 88(4) wt.-% according to the refinement of all five samples. The inset shows the crystal structure of Zr_2Ir_6B emphasizing the alternating filled BIr_6 octahedra (yellow) and empty Ir_6 octahedra (blue). (For interpretation of the references to colour in this figure legend, the reader is referred to the web version of this article.)

There is only one previous solid-state NMR study (in 2002) on perovskite borides [7], which focused on the influence of the boron concentration in the simple cubic compound $ScRh_3B_{1-x}$. However, the existence of the superstructure was not discovered until 2006 and no sample with $x = 0.5$ has been prepared. Herein, we analyzed NMR spectra and spin-lattice relaxation rates with respect to temperature to gain further insights into the underlying mechanisms. Additionally, we report the first microscopic study of Zr_2Ir_6B accounting for the presence of defects and their influence on the density of states. The results obtained by ^{11}B NMR are linked to the band structure and density of states from *ab initio* calculations in order to explain and verify the findings.

2. Experimental

2.1. Ab-initio calculations

The ab-initio total energy and molecular dynamics program "Vienna Ab-initio Simulation Package" (VASP) [21] was used for electronic optimization with the projector-augmented wave (PAW) method [22]. Exchange and correlation in this density functional theory (DFT)-based method were treated with the generalized density approximation (GGA) as parameterized by Perdew, Burke and Entzerhof [23] using an energy cut-off of 500 eV for the plane waves. The experimental lattice parameters and atomic positions were used. The k-mesh was chosen to be $8 \times 8 \times 8$ and built up via the Monkhorst-Pack algorithm [24]. The Bader charge analysis was based on a VASP calculation followed by calculations with the Bader program developed by the Henkelman group [25–27]. The electronic band structure analysis was carried out using the tight-binding, linear muffin-tin orbitals with the atomic spheres approximation (TB-LMTO-ASA) [28–30] as implemented in the TB-LMTO 4.7 program [31]. Exchange and correlation were treated with the GGA functional as parameterized by Perdew and Wang [32]. The k-mesh was $11 \times 11 \times 11$, which leads to 56 k-points in the irreducible Brillouin zone (IBZ). The radii of the automatically generated Wigner-Seitz cells for Zr, Ir and B were 1.93 Å, 1.33 Å and 1.02 Å, respectively. As there is no close packing of the atoms in Zr_2Ir_6B, empty spheres were needed for the LMTO calculations. The bonding analysis was done by calculating the density-of-states (DOS) and the bands in the IBZ. The Fermi level was set to 0 eV as a reference.

2.2. Synthesis

Polycrystalline powder samples of the compound Zr_2Ir_6B were synthesized by arc melting the respective stoichiometric ratio of the elements. To obtain a sufficient sample volume, the procedure below was repeated six times. Each individual powder sample was checked by X-ray powder diffraction to ensure a successful synthesis and to guarantee the purity of the final mixture. The starting materials were powders of zirconium (99.9%, Alfa Aesar) and iridium (99.95%, Alfa Aesar) with the natural isotopic ratios. For boron, a 1:1 mixture of ^{11}B and ^{10}B was used in the synthesis, which was achieved by preparing every sample with 5.56 at.-% of both ^{11}B and ^{10}B (both >96%, Ceradyne, Inc.). Those powders of the elements were mixed, pressed into pellets and arc-melted several times to ensure good homogeneity of the samples. The argon was purified over a silica gel, molecular sieves and a titanium sponge (950 K). The second electrode of the arc furnace was selected to be a tungsten tip in order to withstand the high temperatures. After the arc melting, the obtained product was stable in air. Weight losses during arc melting were negligible. The beady, silver-like product with metallic luster was ground to a fine powder in an agate mortar.